# Thermodynamic properties of $Bi_2Sr_2CaCu_2O_8$ calculated from the electronic dispersion.

J.G. Storey[1], J.L. Tallon[1,2], G.V.M. Williams[2]

[1]*School of Chemical and Physical Sciences, Victoria University, P.O. Box 600, Wellington, New Zealand and*
[2]*MacDiarmid Institute, Industrial Research Ltd., P.O. Box 31310, Lower Hutt, New Zealand*
(Dated: February 1, 2008)

The electronic dispersion for $Bi_2Sr_2CaCu_2O_{8+\delta}$ has been determined from angle-resolved photoelectron spectroscopy (ARPES). From this dispersion we calculate the entropy and superfluid density. Even with no adjustable parameters we obtain an exceptional match with experimental data across the entire phase diagram, thus indirectly confirming both the ARPES and thermodynamic data. The van Hove singularity is crossed in the overdoped region giving a distinctive linear-in-$T$ temperature dependence in the superfluid density there.

PACS numbers: 74.25.Bt, 74.25.Jb, 74.62.Dh, 74.72.-h

The generic doping dependence of the thermodynamic, electrodynamic and transport properties of high-$T_c$ superconductors remains a puzzle despite many years of study. Their unusual behaviour is often taken to be a signature of exotic physics yet it should be related to the electronic energy-momentum dispersion, obtained for example from angle-resolved photoemission spectroscopy (ARPES). These studies indicate the presence of an extended van Hove saddle-point singularity[1] situated at the $(0,\pi)$ point together with a normal-state pseudogap[2] as common features in the electronic band structure of the cuprate superconductors. The pseudogap exhibits a reduction in the density of states (DOS) at the Fermi level which is believed to develop into a fully nodal gap at low temperature[3].

In theories based on the so-called van Hove scenario[4] the superconducting (SC) transition temperature, $T_c$, is enhanced by the close proximity of a van Hove singularity (vHs). These theories assume that the vHs sweeps through the Fermi level at around optimal doping ($p = 0.16$), indeed causing the peak in $T_c(p)$. However, ARPES measurements of the band structure of Bi-2201[5] show that the vHs crosses the Fermi level in the deeply overdoped side of the phase diagram. For a bilayer cuprate like Bi-2212 the weak coupling between the layers splits the bands near the $(\pi, 0)$ points into an upper antibonding band and a lower bonding band. ARPES measurements performed on Bi-2212[6] suggest that the antibonding band vHs crosses at around $p = 0.225$ where $T_c \approx 60$K i.e. near the limit for overdoping in this material. The vHs crossing should profoundly affect all physical properties.

In this work we have used the thermodynamic properties as a window on the electronic structure to independently check the main ARPES results. Using an ARPES-derived energy dispersion we have calculated the doping and temperature dependence of the entropy and superfluid density of Bi-2212. All details for our calculations are taken directly, and only, from ARPES in order to determine the implications of this data. Our calculations confirm the ARPES results, giving a consistent picture of the thermodynamic and electrodynamic properties in terms of a proximate vHs.

We assume Fermi-liquid-like, mean-field, weak-coupling physics in spite of indications, or expectations, to the contrary. In defense of our approach (i) the thermodynamics at low $T$ is dominated by the nodal regions of the Fermi surface where quasiparticles are well defined and long lived; and (ii) the Wilson ratio relating spin susceptibility to $S/T$ (where $S$ is the electronic entropy) is almost exactly that for nearly free electrons across a wide range of doping and temperature[7]. Moreover, the non-mean-field BCS-like behaviour is generally inferred from the unusual $2\Delta/k_B T_c$ ratio which grows with underdoping. But it has always been our view[8], and is now confirmed[9, 10] that the large and growing energy gap used here is the $(\pi,0)$ pseudogap, not the SC gap. Once the pseudogap is properly included in the problem then $2\Delta/k_B T_c$ is well behaved. We do not treat fluctuations which are confined to $T_c \pm 15$K[11] and are a minor embellishment.

For Bi-2212 we employ a 2D bilayer dispersion $\epsilon_{\mathbf{k}}$ provided by the authors of ref. [6], which was obtained from tight binding fits to high-resolution ARPES data. The DOS per spin at energy $E$ is given by

$$N(E) = N_k^{-1} \sum_{\mathbf{k}} \delta\left(\epsilon_{\mathbf{k}} - E\right) \quad (1)$$

The entropy per mole $S$ for weakly interacting fermions is given by[12]

$$S = -2R \int [f \ln f + (1 - f) \ln(1 - f)] N(E) dE \quad (2)$$

where $f$ is the Fermi-Dirac distribution function and $R$ is the gas constant. The chemical potential $\mu(T)$ is calculated self-consistently such that the carrier concentration $n$ is $T$-independent. $n$ is given by:

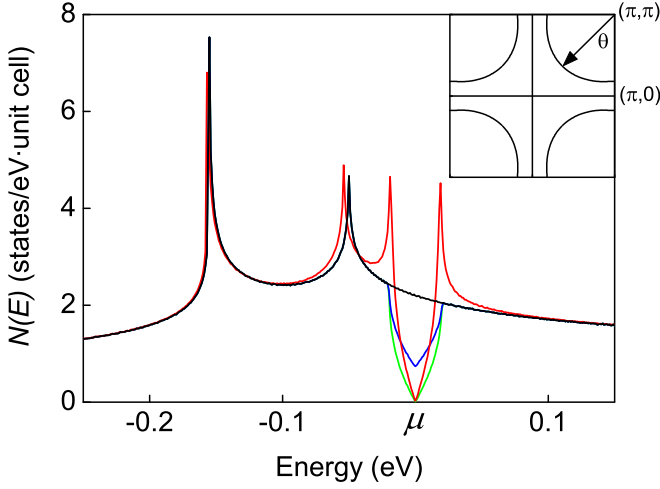$$n = (2/V_A) \int f(E) N(E) dE \quad (3)$$

FIG. 1: (Color) The DOS calculated from the Bi-2212 bilayer dispersion determined by ARPES measurements (black). Also shown is a 20meV pseudogap at 0K (green) and 100K (blue), and a 20meV SC gap at 0K (red). Inset: the Fermi surface in the $(k_x, k_y)$ plane showing the angle $\theta$.

Where $V_A$ is the atomic volume per formula unit.

The Fermi surface (FS) in the 1st Brillouin Zone is shown in the inset to Fig. 1. The pseudogap first forms on the FS near $(\pi, 0)$ leaving ungapped Fermi arcs[13] between. With decreasing temperature the Fermi arcs narrow such that the gap seems to become nodal at $T = 0$. We therefore adopt a pseudogap of the form

$$
E_g = \begin{cases} E_{g,max} \cos\left(\frac{2\pi\theta}{4\theta_0}\right) & (\theta < \theta_0) \\[2mm] E_{g,max} \cos\left(\frac{2\pi(\theta - \pi/2)}{4\theta_0}\right) & (\theta > \frac{\pi}{2} - \theta_0) \\[2mm] 0 & \text{otherwise} \end{cases} \quad (4)
$$

where

$$
\theta_0 = \frac{\pi}{4}\left(1 - \tanh\left(\frac{T}{T^*}\right)\right) \quad (5)
$$

and $T^* = E_{g,max}/k_B$. $\theta$ is the angle shown in Fig. 1.

Eqn. 5 models the observed temperature dependence of the Fermi arc length[3]. At $T = 0$, $\theta_0 = \pi/4$ and the pseudogap is fully nodal. As $T$ rises, $\theta_0$ decreases resulting in a 'filling-in' of the pseudogap and the growth of the Fermi-arcs. This model is based on results by Kanigel et al.[3] that show the Fermi-arcs collapsing linearly as a function of $T/T^*$, extrapolating to zero as $T \to 0$. However we note an important feature of our model. The Kanigel data shows the pseudogap opening abruptly at $T = T^*$. A pseudogap which fills completely at $T^*$ would result in a jump in the specific heat coefficient $\gamma$ at $T^*$, which is not observed. The smooth evolution of the tanh function in Eqn. 5 overcomes this problem. The pseudogap is states-non-conserving i.e. unlike the SC gap there

is no pile up of states outside the gap (see Fig. 1). This is implemented by eliminating states with energies $E < E_g$ from the summations.

Fig. 1 shows the DOS calculated from the bilayer dispersion. The bonding and antibonding band vHs's are clearly visible with the former 105meV below the latter. Also shown is a 20meV pseudogap at $T = 0$K and 100K illustrating the gap filling with temperature. The gap node is pinned to the chemical potential at all $T$.

The entropy in the SC state has been modelled using a $d$-wave gap of the form $\Delta_{\mathbf{k}} = \frac{1}{2}\Delta_0 g_{\mathbf{k}}$ where $g_{\mathbf{k}} = \cos k_x - \cos k_y$. The dispersion in the presence of the SC gap is given by $E_{\mathbf{k}} = \sqrt{\epsilon_{\mathbf{k}}^2 + \Delta_{\mathbf{k}}^2}$ and $\Delta_0(T)$ is determined from the self-consistent weak-coupling BCS gap equation[12]

$$
1 = \frac{V}{2}\sum_{\mathbf{k}} \frac{|g_{\mathbf{k}}|^2}{E_{\mathbf{k}}} \tanh\left(\frac{E_{\mathbf{k}}}{2k_B T}\right) \quad (6)
$$

We adopt a pairing potential of the form $V_{\mathbf{k}\mathbf{k'}} = V g_{\mathbf{k}} g_{\mathbf{k'}}$. The amplitude, $V$, is assumed to be constant (=125meV) up to an energy cut-off, $\omega_c$, chosen such that $T_c$ matches the experimentally observed value. The pseudogap is not included in the process of calculating $\Delta_0(T)$.

The superfluid density, $\rho_s$, is proportional to the inverse square of the penetration depth given by[14]

$$
\begin{aligned}
\frac{1}{\lambda_{ab}^2} &= \frac{\mu_0 e^2 n}{4\pi\hbar^2}\sum_{\mathbf{k}}\left[\left(\frac{\partial\epsilon_{\mathbf{k}}}{\partial k_x}\right)^2 \frac{\Delta_{\mathbf{k}}^2}{E_{\mathbf{k}}^2} - \frac{\partial\epsilon_{\mathbf{k}}}{\partial k_x}\frac{\partial\Delta_{\mathbf{k}}}{\partial k_x}\frac{\Delta_{\mathbf{k}}\epsilon_{\mathbf{k}}}{E_{\mathbf{k}}^2}\right] \\
&\times \left[\frac{1}{E_{\mathbf{k}}} - \frac{\partial}{\partial E_{\mathbf{k}}}\right]\tanh\left(\frac{E_{\mathbf{k}}}{2k_B T}\right) \quad (7)
\end{aligned}
$$

The summation in Eqs. 6 and 7 is performed over both the bonding and anti-bonding bands and $\Delta$ is assumed to be the same for both bands[15].

The data points in Fig. 2(a) show the normal- and SC-state entropy data of Loram et al[7]. Fig. 2(b) shows the absolute entropy calculated, as described, from the dispersion with no fitting parameters. We have merely specified the location of $E_F$ relative to $E_{vHs}$ at two points only: in the overdoped region from Kaminski et al.[6] and in the underdoped region from Kordyuk et al.[16] and interpolated between. The overall $T$- and doping-dependence of the experimental data is reproduced superbly, with absolute values just a factor of $3/4$ lower. This is our first main result. $S/T$ rises with doping and reaches its maximum at the vHs (as observed also in $\mathrm{La}_{2-x}\mathrm{Sr}_x\mathrm{CuO}_4$[7]). A similar effect is seen in the spin susceptibility[7] and Knight shift[11]. In Fig. 2(a) we have rescaled the computed entropy by the constant factor of $4/3$ and refined the fit by using $E_F$ and $E_{g,max}$ as fitting parameters. These refinements do not alter the overall behaviour and are tightly constrained. For example, the normal-state fits to the four most overdoped data sets have been obtained by adjusting a single parameter, namely $E_F$, as are the high-$T$ asymptotes for all data
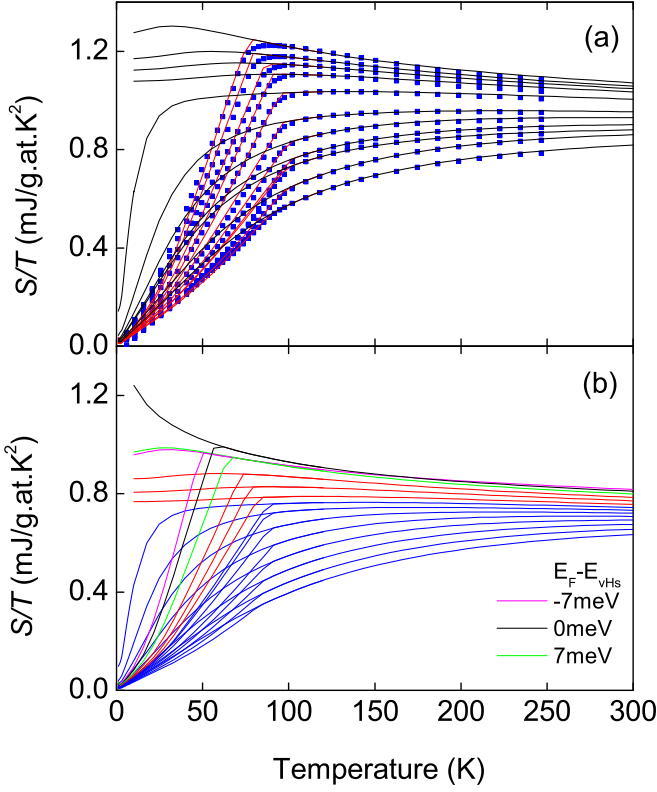
FIG. 2: (Color) (a) Refined normal-state (black) and SC-state (red) fits to the electronic entropy data of Loram *et al*[7] for Bi-2212. For clarity every 20th data point only is shown. Each curve represents a different doping level from $p = 0.129$ to 0.209. (b) Unrefined absolute entropy curves with no fitting parameter.
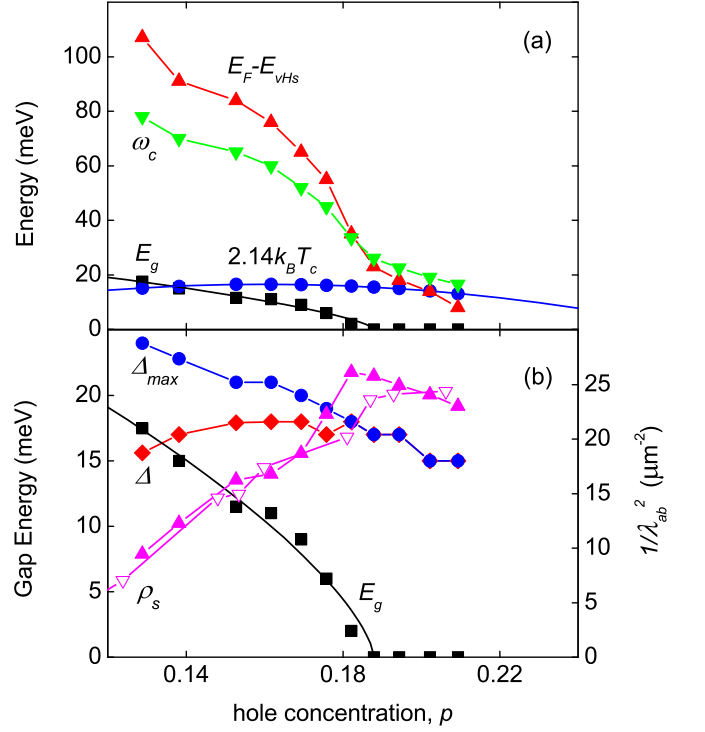


FIG. 3: (Color) (a) $E_F - E_{vHs}$ (up triangles). The vHs will cross $E_F$ at $p \approx 0.22$. Pairing potential energy cut-off $\omega_c$ (down triangles). Pseudogap magnitude $E_g$ (squares) and a fit given by Eqn. 8. The measured $T_c$ multiplied by $2.14k_B$ (circles). (b) Maximum gap as measured from the DOS at 10K (circles). SC gap measured from the DOS at 10K in the absence of a pseudogap (diamonds). Calculated super-fluid density at 10K (up triangles). Measured low-$T$ Bi-2212 superfluid density[21] (down triangles).

sets. The Fermi level in the most overdoped fit is only 8meV above the antibonding band vHs.

As the doping decreases the vHs recedes from $E_F$ resulting in a decrease in the number of states within $k_B T$ of $\mu$ and a corresponding reduction in entropy. However as the doping is further reduced the recession of the vHs from $E_F$ is no longer able to account for the observed decrease in entropy alone and the second adjustable parameter, the pseudogap magnitude $E_g$, is introduced. This results in the progressive downturn in the normal state $S/T$ as temperature decreases. The deduced values of $E_F - E_{vHs}$ and $E_g$ are plotted versus doping in Fig. 3(a) along with the measured $T_c$. The doping level has been determined from the empirical relation[17] $p = 0.16 \pm 0.11\sqrt{1 - T_c/T_{c,max}}$. The fits suggest that the antibonding vHs will cross $E_F$ near $p = 0.22$ in full agreement with recent ARPES studies[6] on Bi-2212 where the crossing occurs at $p = 0.225$. This is our next key result.

The pseudogap is observed to open at critical doping $p_{crit} = 0.188$ in agreement with previous analyses[7, 18]. $E_g$ has been fitted with the following equation

$$T^*(p) = E_g/k_B = T_0^* \left(1 - p/p_{crit}\right)^{1-\alpha} \qquad (8)$$

with $T_0^* = 443.7$K and $\alpha = 0.317$. These values agree with the results of Naqib *et al.*[19] who determined $T^*(p)$ of YBCO from transport studies. A fit to their data gives $T_0^* = 510$K and $\alpha = 0.2$. The sublinear behavior of $T^*(p)$ is expected if $p_{crit}$ is a quantum critical point[20].

From the SC state fits the energy cutoff, $\omega_c$, is, surprisingly, found to be linearly related to $E_F - E_{vHs}$. In particular $\omega_c(meV) = 10.96 + 0.637(E_F - E_{vHs})$ with correlation coefficient $R = 0.99945$. The rapid fall in $\omega_c$ is suggestive of magnetic or magnetically enhanced pairing, rather than phononic.

Fig. 3(b) shows the magnitude of the combined SC gap and pseudogap, $\Delta_{max}$, measured from the calculated DOS at 10K. $\Delta_{max}$ increases with decreasing doping just as observed from ARPES[22], tunnelling[23] and Raman scattering[24]. Also plotted is the SC gap magnitude $\Delta$, determined by setting $E_g = 0$ and measuring the gap in the calculated DOS at 10K. The magnitude is smaller than typically observed because of the weak coupling assumption for which $2\Delta/k_B T_c = 4.28$. The gap, $\Delta$, rises and falls in conjunction with the observed $T_c$. Note that the experimentally observed monotonic increase in the

gap magnitude with decreasing doping is here seen to be associated with the pseudogap, and not the SC gap as generally believed. The behaviour here is consistent with the two-gap picture presented by Deutscher[25] and more recently by Le Tacon *et al.*[10] but has been a feature of our work for a long time[8, 18, 26].

Using the parameters obtained from the entropy fits the superfluid density has been calculated using Eqn. 7 with no further adjustable parameters, and is shown in Fig. 4(a). For comparison (and in the absence of data for Bi-2212) Fig. 4(b) shows the $ab$-plane superfluid density of $La_{2-x}Sr_xCuO_4$ (La-214) determined by ac-susceptibility measurements[27] on grain-aligned samples. There is excellent agreement. The increasing linearity of $\rho_s(T)$ with overdoping can now be understood in terms of the approach to the vHs where full linearity occurs. (The crossing of the vHs in La-214 can also be inferred from the maximum in the entropy at $p = 0.24$[7].) The opening of the pseudogap leads to the strong reduction in $\rho_s$ observed below $p = 0.19$. This is clearly illustrated by the plot of $\rho_s(10K)$ vs $p$ in Fig. 3(b). The overall doping dependence and absolute magnitude of $\rho_s(10K)$ concurs almost exactly with experimental data for Bi-2212[21] also shown in Fig. 3(b). This is our third key result. We recall that no fitting parameters are used in Eqn. 7. It is remarkable that $S/T$ and $\rho_s(T)$ are so similar in La-214, Bi-2212 and indeed $Y_{1-x}Ca_xBa_2Cu_3O_{7-\delta}$, despite the significant differences in bare band structure. The renormalised dispersion near $E_F$ seems to lead to a universal phenomenology which calls for theoretical explanation.

In the underdoped data the downturn seen at low $T$ and $p$ in the calculated $\rho_s(T)$ curves arises from the closing of the Fermi arcs and is not observed in the experimental data which show an upturn at low $T$ and $p$. A similar downturn would occur in the condensation energy, which again is not observed. To us this indicates that the Fermi arc picture is, at best, incomplete. We will discuss this elsewhere.

In summary, we have calculated the entropy and superfluid density of Bi-2212 directly from an ARPES-derived energy-momentum dispersion. The temperature and doping dependence of both the entropy and superfluid density can be fully explained by the combined effects of a proximate vHs and the opening of a normal-state pseudogap. These results provide indirect confirmation of both the thermodynamic and low-energy ARPES data. Fits to Bi-2212 entropy data indicate that the antibonding vHs crosses the Fermi level near $p = 0.22$ in agreement with recent ARPES results. The superfluid density calculated using no adjustable parameters shows excellent agreement with experimental data and exhibits a distinctive overall linear-in-$T$ behaviour at the vHs. The universal renormalised phenomenology in the various cuprates, despite their differences in bare band structure, is a key conclusion that demands theoretical
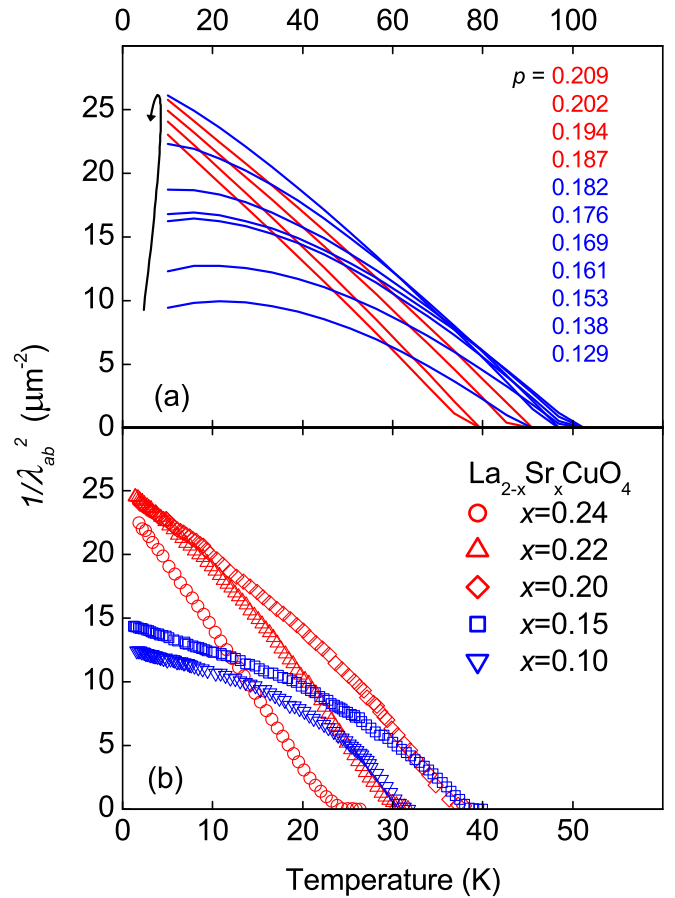


FIG. 4: (Color) (a) Superfluid density computed using paramaters from the entropy fits in Fig. 2. The arrow points in the direction of increasing doping. Curves/data in which the pseudogap is present are shown in blue. (b) Superfluid density of La-214 obtained from ac-susceptibility measurements [27]

explanation. It also remains a theoretical challenge to understand why the Fermi-liquid approach is so successful in a strongly-correlated system.

[1] J. Ma, C. Quitmann, R. J. Kelley, P. Almeras, H. Berger, G. Margaritondo, and M. Onellion, Phys. Rev. B **51**, 3832 (1995).

[2] H. Ding, T. Yokoya, J. C. Campuzano, T. Takahashi, M. Randeria, M. R. Norman, T. Mochiku, K. Kadowaki, and J. Giapintzakis, Nature **382**, 51 (1996).

[3] A. Kanigel, M. R. Norman, M. Randeria, U. Chatterjee, S. Souma, A. Kaminski, H. M. Fretwell, S. Rosenkranz, M. Shi, T. Sato, et al., Nature Physics **2**, 447 (2006).

[4] R. S. Markiewicz, J. Phys. Chem. Solids **58**, 1179 (1997).

[5] T. Kondo, T. Takeuchi, T. Yokoya, S. Tsuda, S. Shin,

and U. Mizutani, J. Electron. Spectrosc. Relat. Phenom. **137**−**140**, 663 (2004).

[6] A. Kaminski, S. Rosenkranz, H. M. Fretwell, M. R. Norman, M. Randeria, J. C. Campuzano, J. M. Park, Z. Z. Li, and H. Raffy, Phys. Rev. B **73**, 174511 (2006).

[7] J. W. Loram, J. Luo, J. R. Cooper, W. Y. Liang, and J. L. Tallon, J. Phys. Chem. Solids. **62**, 59 (2001).

[8] J. L. Tallon and J. W. Loram, Physica C **349**, 53 (2001).

[9] K. Tanaka, W. S. Lee, D. H. Lu, A. Fujimori, T. Fujii, Risdiana, I. Terasaki, D. J. Scalapino, T. P. Devereaux, Z. Hussain, et al., Science **314**, 1910 (2006).

[10] M. Le Tacon, A. Sacuto, A. Georges, G. Kotliar, Y. Gallais, D. Colson, and A. Forget, Nature Physics **2**, 537 (2006).

[11] J. W. Loram, J. L. Tallon, and W. Y. Liang, Phys. Rev. B **69**, 060502 (2004).

[12] R. D. Parks, *Superconductivity* (Marcel Dekker, New York, 1969), vol. 1.

[13] M. R. Norman, H. Ding, M. Randeria, J. C. Campuzano, T. Yokoya, T. Takeuchi, T. Takahashi, T. Mochiku, K. Kadowaki, P. Guptasarma, et al., Nature **392**, 157 (1998).

[14] D. E. Sheehy, T. P. Davis, and M. Franz, Phys. Rev. B **70**, 054510 (2004).

[15] S. V. Borisenko, A. A. Kordyuk, T. K. Kim, S. Legner, K. A. Nenkov, M. Knupfer, M. S. Golden, J. Fink, H. Berger, and R. Follath, Phys. Rev. B **66**, 140509 (2002).

[16] A. A. Kordyuk, S. V. Borisenko, M. Knupfer, and J. Fink, Phys. Rev. B **67**, 064504 (2003).

[17] M. R. Presland, J. L. Tallon, R. G. Buckley, R. S. Liu, and N. E. Flower, Physica C **176**, 95 (1991).

[18] J. L. Tallon, G. V. M. Willams, M. P. Staines, and C. Bernhard, Physica C **235-240**, 1821 (1994).

[19] S. H. Naqib, J. R. Cooper, J. L. Tallon, R. S. Islam, and R. A. Chakalov, Phys. Rev. B **71**, 054502 (2005).

[20] J. Zaanen and B. Hosseinkhani, Phys. Rev. B **70**, 060509(R) (2004).

[21] W. Anukool, Ph.D. thesis, U. of Cambridge, England (2003).

[22] J. C. Campuzano, H. Ding, M. R. Norman, H. M. Fretwell, M. Randeria, A. Kaminski, J. Mesot, T. Takeuchi, T. Sato, T. Yokoya, et al., Phys. Rev. Lett. **83**, 3709 (1999).

[23] N. Miyakawa, P. Guptasarma, J. F. Zasadzinski, D. G. Hinks, and K. E. Gray, Phys. Rev. Lett. **80**, 157 (1997).

[24] C. Kendziora and A. Rosenberg, Phys. Rev. B **52**, 9867 (1995).

[25] G. Deutscher, Nature **397**, 410 (1999).

[26] J. Loram, K. A. Mirza, J. R. Cooper, W. Y. Liang, and J. M. Wade, J. Supercon. **7**, 243 (1994).

[27] C. Panagopoulos, B. D. Rainford, J. R. Cooper, W. Lo, J. L. Tallon, J. W. Loram, J. Betouras, Y. S. Wang, and C. W. Chu, Phys. Rev. B **60**, 14617 (1999).